Molecular Therapy
Oncolytics
Original Article

Artificial T Cell Adaptor Molecule-Transduced TCR-T Cells Demonstrated Improved Proliferation Only When Transduced in a Higher Intensity

Toshiyasu Sakai,[1] Seitaro Terakura,[1] Kotaro Miyao,[1] Shingo Okuno,[1] Yoshitaka Adachi,[1] Koji Umemura,[1] Jakrawadee Julamanee,[1,2] Keisuke Watanabe,[1,3] Hiroshi Hamana,[4] Hiroyuki Kishi,[4] Judith Leitner,[5] Peter Steinberger,[5] Tetsuya Nishida,[1] Makoto Murata,[1] and Hitoshi Kiyoi[1]

[1]Department of Hematology and Oncology, Nagoya University Graduate School of Medicine, Nagoya, Japan; [2]Division of Clinical Hematology, Faculty of Medicine, Prince of Songkla University, Songkhla, Thailand; [3]Division of Cancer Immunology, National Cancer Center Research Institute, Tokyo, Japan; [4]Department of Immunology, Faculty of Medicine, Academic Assembly, University of Toyama, Toyama, Japan; [5]Division for Immune Receptors and T Cell Activation, Institute of Immunology, Medical University of Vienna, Vienna, Austria

An artificial T cell adaptor molecule (ATAM) was generated to improve persistence of T cell receptor (TCR) gene-transduced T (TCR-T) cells compared to such persistence in a preceding study. ATAMs are gene-modified CD3ζ with the intracellular domain of 4-1BB inserted in the middle of CD3ζ. NY-ESO-1 TCR-T cells transduced with an ATAM with two separated virus vectors demonstrated superior proliferation upon antigen stimulation. To further develop clinically applicable ATAM-transduced TCR-T cells, we attempted to make a single virus vector to transduce the TCR and ATAM simultaneously. Because we failed to observe improved proliferation capacity upon stimulation after one virus vector (1vv) transduction, we compared TCR-T cells transduced with 1vv and two virus vector (2vv) methods to elucidate the reason. In Jurkat reporter cells, an ATAM transduced by the 2vv method demonstrated a higher intensity than by the 1vv method, and the ATAM intensity was associated with increased nuclear factor κB (NF-κB) signals upon stimulation. In ATAM-transduced primary T cells, a transduced ATAM by the 2vv method showed higher intensity and better proliferation. ATAM-transduced TCR-T cells demonstrated improved proliferation only when the ATAM was transduced at a higher intensity. To create a simpler transduction method, we need to develop a strategy to make a higher ATAM expression to prove the efficacy of ATAM transduction in TCR-T therapy.

INTRODUCTION

Endogenous or gene-modified T cells with antigen-specific T cell receptors (TCRs) demonstrated certain clinical benefits, and they represent one of the major approaches for cytotoxic T lymphocyte (CTL) therapies.[1–4] Because of the difficulties of endogenous tumor-specific CTL generation, the introduction of tumor-specific TCRs to polyclonal T cells has become a mainstay to generate CTLs with tumor-specific TCR (TCR-CTLs).[5,6] However, gene-modified TCR-CTL therapies targeting malignant tumors have been generally unsuccessful in previous clinical trials.[5,7,8] One of the major reasons for this was considered to be poor expansion and short persistence of the transferred CTLs.[9] To overcome these problems, we have previously developed an artificial T cell adaptor molecule (ATAM), which is a gene-engineered *CD3ζ (CD247)* containing either a CD28 or 4-1BB intracellular domain (ICD).[10] It was developed to mimic the ICD of chimeric antigen receptor (CAR) T cells.[11,12] After TCR and peptide-human leukocyte antigen (HLA) ligation, CD3ζ is recruited to the TCR complex via its ionized transmembrane residues, forms a supramolecular activation cluster, and downstream activation signals are delivered to the CTLs by several endogenous adaptor molecules, such as CD3ζ, Lck, ZAP70, and others.[13–15] Thus, we focused on enhancing the downstream activation signals after TCR epitope ligation, and demonstrated improved intracellular signaling by modifying the adaptor molecule component of the complex, particularly with an adaptor molecule including the 4-1BB ICD.

The idea of ICD modification originated from CAR gene-modified T cells and their great success. During the development of CAR-T cell therapy, after the introduction of ICDs for co-stimulatory molecules, such as CD28 or 4-1BB, the second-generation CARs have shown improved proliferation and persistence, and subsequent clinical efficacy.[12,16] Thus, we obtained a similar approach in TCR-CTLs by incorporating an ICD in the middle of the CD3ζ molecule. Upon conducting the present study to a make simpler method to introduce the TCR and ATAM into T cells, we designed TCR α and β chains directly linked to an ATAM molecule at first. However, those moieties could not be successfully transduced and expressed as a correct TCR conformation on the T cells (data not shown). In the

Received 19 June 2020; accepted 26 August 2020;
https://doi.org/10.1016/j.omto.2020.08.014.

Correspondence: Seitaro Terakura, MD, PhD, Department of Hematology and Oncology, Nagoya University Graduate School of Medicine, 65 Tsurumai-cho, Showa-ku, Nagoya, Aichi 466-8560, Japan.
E-mail: tseit@med.nagoya-u.ac.jp

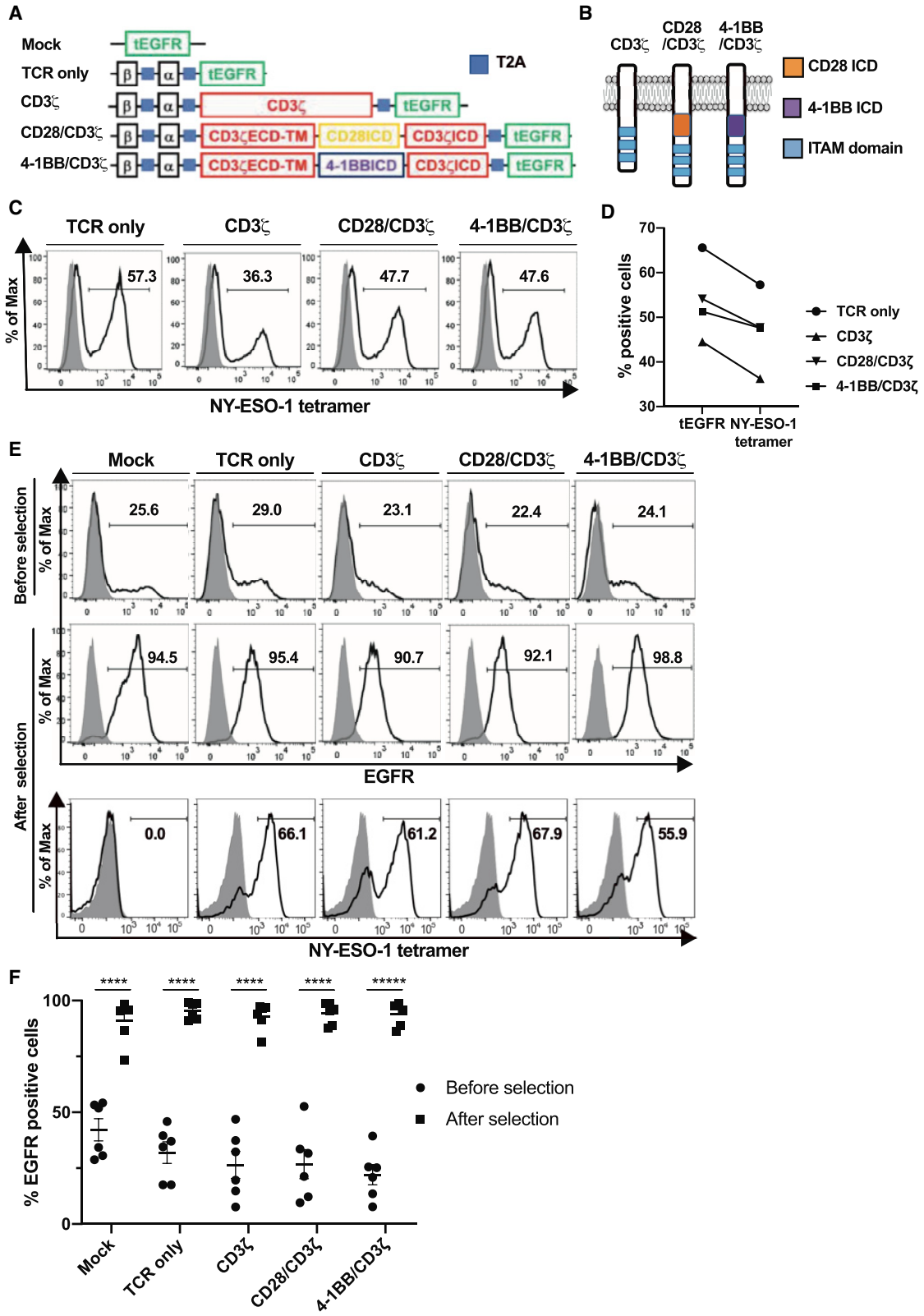

(legend on next page)

preceding study, we designed a novel adaptor molecule based on CD3ζ, which is inserted with either the CD28 or 4-1BB ICD, to enhance signaling after TCR ligation to specific epitopes. We transduced these novel adaptor molecules into endogenous and TCR genetically modified T cells and examined various T cell functions, including proliferation upon stimulation *in vitro* and *in vivo*. We successfully demonstrated the potential for increasing proliferation capacity of TCR-CTL therapy using novel adaptor molecules consisting of CD3ζ and 4-1BB ICDs.[10]

Herein, we attempted to further develop an all-in-one virus vector that can transduce a tumor-specific TCR and the artificial T cell adaptor molecule (ATAM) in a single transduction. We aimed to develop feasible and useful methods to transduce the TCR and ATAM to the patients' peripheral blood-derived T cells. Indeed, we could not reproduce the boosting effect of an ATAM using the single virus vector. However, we found that it is important to realize a higher ATAM intensity as well as TCR to convey the boosting effect of an ATAM.

RESULTS

Generation of TCR and ATAMs and Their Expression in Transduced Cells

In the previous study, we chose NY-ESO-1 TCR as a TCR-T model, and transduced the ATAM simultaneously by two separated virus vectors (two virus vector method [2vv method]).[10] To transduce the TCR and ATAMs in a further simplified method, we attempted to develop a single virus vector, by which we can transduce the TCR and ATAM in one gene transduction into T cells (one virus vector method [1vv method]). We designed cDNAs that encode TCR-ATAMs and co-expressing a truncated version of the epidermal growth factor receptor (tEGFR) (Figures 1A and 1B). To confirm whether we could successfully transduce the TCR-ATAMs into target cells, we transduced SUP-T1 cells by using retrovirus vectors (Figures 1C and 1D). We observed that SUP-T1 cells transduced with TCR-ATAM-tEGFR could build the conformationally correct TCR component, were recognized by the HLA-A2-NY-ESO-1 tetramer, and co-expressed tEGFR as a transduction marker. Expression of NY-ESO-1 TCR and EGFR was almost equivalent, and was similar among various constructs.

Establishment of the ATAM+NY-ESO-1 TCR-CTL Model

To investigate the effect of ATAM transduction in the context of the antitumor effect of TCR-CTL therapy, we transduced TCR-ATAM-tEGFR into primary human $CD8^+$ T cells by the 1vv method. ATAMs were transduced on days 3 and 4 of CD3/CD28 beads stimulation, and then tEGFR selection was performed on day 7. Transduction efficiencies were approximately 20% (range, 8%–55%) before tEGFR selection. After immunomagnetic selection, the $tEGFR^+$ cells were purified up to 73%–99% (Figures 1E and 1F). Purified TCR-CTLs were NY-ESO-1 tetramer positive at slightly lower percentages compared with tEGFR positivity. This phenomenon was probably because of the TCR mispairing between the endogenous TCR and exogenously inserted TCR.[17–19] The percentages of NY-ESO-1 $tetramer^+$ cells were slightly varied by individual donor, whereas the percentages of $tetramer^+$ cells were similar among various constructs. Purified TCR-CTLs were cryopreserved on day 11. Upon usage, CTLs were thawed, restimulated, and expanded to apply for the downstream experiments.

Cytokine Production, Cell Proliferation, and Cytotoxicity of ATAM+NY-ESO-1 TCR-CTLs

To evaluate the anti-tumor recognition capacity of ATAM+TCR-CTLs, we performed intracellular cytokine assay against K562-HLA-A2 cells pulsed with NY-ESO-1 peptide. Proportions of positive responders were similar for interferon (IFN)-γ and interleukin (IL)-2 among CTLs transduced with a TCR only and ATAM+TCR-CTLs (Figures 2A and 2B). IFN-γ and IL-2 secreted by CTLs transduced TCR only, and ATAM+TCR-CTLs were further determined in the supernatant using ELISA. ATAM+TCR-CTLs were cocultured with K562-HLA-A2 cells pulsed with or without NY-ESO-1 peptide. No additional increase in cytokine production was observed with the transduction of ATAMs (Figure 2C).

Next, we investigated *in vitro* expansion of ATAM+NY-ESO-1 TCR-CTLs after a single course of antigen stimulation at a 1:1 ratio with gamma-irradiated K562-HLA-A2 cells pulsed with NY-ESO-1 peptide. No significant difference of cell proliferation was observed (Figure 2D). To evaluate the integrated response including specific cytotoxicity and proliferation to $NY\text{-}ESO\text{-}1^+$ targets, we performed a coculture assay. MM.1S-HLA-A2 cells were used as the target cells, and the effector cells were mock or CTL-transduced TCR only and ATAM+TCR-CTLs. Effector and stimulator cells were cocultured at various effector-to-target (E:T) ratios and incubated for a total of 120 h, assessing the percentage of CTLs and MM.1S cells by flow cytometry every 24 h. Both under short-term incubation up to 48 h and long-term incubation up to 120 h, TCR only and ATAM+TCR-CTLs showed similar E:T cell proportions under both E:T ratio conditions (1:1 and 1:8) (Figures 2E and 2F). In the lower target cell ratio (E:T ratio of 1:1), we observed a relatively higher T cell proportion even

Figure 1. Generation of ATAMs and Gene Transduction into Cell Lines and Primary T Cells

(A) Schematic representation of the TCR-T and ATAM constructs. Blue square indicates T2A sequence. β, TCR β chain; α, TCR α chain; ECD, extracellular domain; TM, transmembrane; ICD, intracellular domain. (B) Schematic of ATAM design on the cell membrane surface. ITAM, immunoreceptor tyrosine-based activation motif. (C) Transduction efficiencies of TCR and ATAMs. Flow cytometry analysis of SUP-T1 cell lines transduced with NY-ESO-1 TCR and ATAMs. Gray histograms represent parallel-stained untransduced SUP-T1 cells. Representative flow plots are shown from two independent experiments with similar results. The number indicates percentages of $tetramer^+$ cells. (D) The percentages of NY-ESO-1 tetramer and EGFR of ATAM-transduced SUP-T1 cells. (E and F) Flow cytometry analysis of $ATAM^+$ $CD8^+$ cells before and after tEGFR selection. Representative flow data are shown in (E), and a summary from six different donors is shown in (F) (paired Student's t test: ****$p < 0.0001$, *****$p < 0.00001$). Data represent means ± SEM.

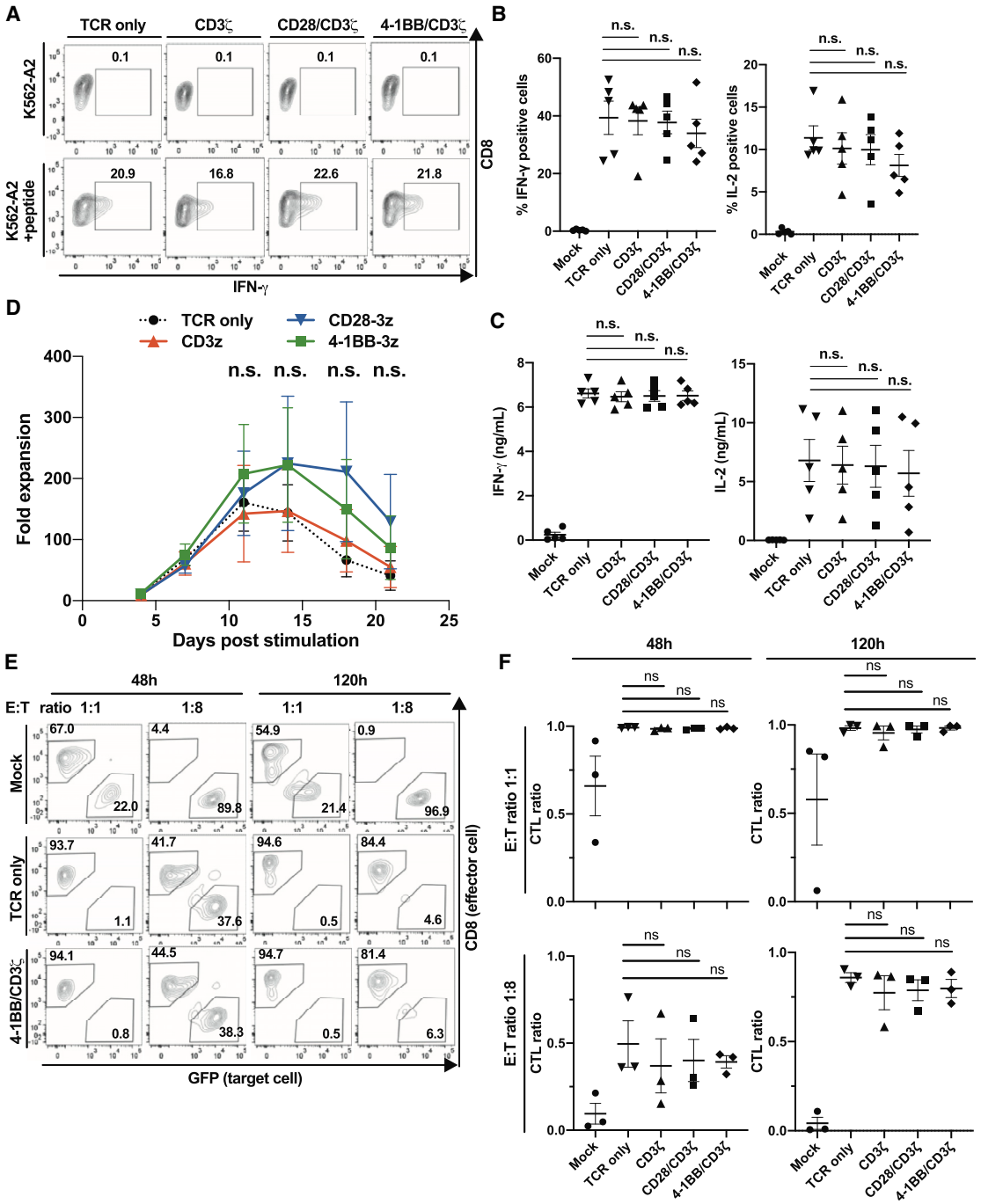

Figure 2. Cytokine Production, Antitumor Effect, and Cell Proliferation of ATAM$^+$ TCR-CTLs

(A and B) Intracellular IFN-γ and IL-2 production after stimulation with K562-HLA-A2 cells pulsed with or without NY-ESO-1 peptide. Representative flow plots are shown in (A), and a summary from five different donors is shown in (B). Data represent means ± SEM (one-way ANOVA: n.s., not significant). (C) The secretion of IFN-γ and IL-2 into the culture supernatant. The stimulators were irradiated HLA-A2$^+$ K562 cells pulsed with NY-ESO-1 peptide. Data represent means ± SEM (one-way ANOVA: n.s.). (D) Proliferation after single antigen stimulation. Data are from the analysis of five different donors. Data represent means ± SEM, and no significant differences were observed (two-way ANOVA: n.s.). (E) Coculture assay between ATAM$^+$ CTLs and EGFP$^+$ MM.1S cells. ATAM$^+$ CTLs were cocultured with nonirradiated MM.1S (originally, an HLA-A2$^-$ and NY-ESO-1$^+$ myeloma cell line) to assess effects on both cytotoxicity and proliferation, at E:T (effector-to-target) ratios of 1:1 or 1:8, and then the percentages of CTLs and

(legend continued on next page)

in the mock T cell group possibly due to natural killer cell activity. In brief, ATAM+TCR-CTLs generated by the 1vv method did not show any advantageous effect with regard to cytokine secretion, cell proliferation, and cytotoxicity to NY-ESO-1$^+$ target cells compared with TCR-CTLs without ATAM.

Expression of ATAM after Different Transduction Methods

In the previous study, we demonstrated that the ATAM with 4-1BB-ICD could exhibit an advantageous effect on the proliferation of TCR-CTLs, whereas the ATAM with CD28-ICD did not have the same effect on cell proliferation as was seen with ATAM with 4-1BB-ICD.[10] However, we could not reproduce the effect in the present study. To investigate the reason why we could not detect the proliferation superiority in the present study, we focused on the transduction methods and compared the TCR-T cells of the 1vv method and those of the 2vv method (Figure 3A). In the previous study, we adopted the 2vv method, which included a simultaneous transduction of TCR-enhanced green fluorescent protein (EGFP) and ATAM-2A-tEGFR (2vv method, Figure 3A). Because the ATAM with CD28-ICD did not enhance the proliferation of transduced cells,[10] we focused onto the ATAM with 4-1BB-ICD in the subsequent experiments. We transduced the TCR and ATAMs into Jurkat cells with either the 1vv or 2vv method. After transduction, tEGFR$^+$ fractions were purified with immunomagnetic beads (Figure 3B). Mean fluorescence intensity (MFI) of tEGFR after 1vv method transduction was lower in CD28/CD3ζ and 4-1BB/CD3ζ ATAMs, whereas the tEGFR or CD3ζ transduction group showed similar levels of tEGFR expression between the 1vv and 2vv method (Figure 3B). In terms of protein expression, we observed consistently lower protein expression after 1vv method transduction, which was particularly lower in the 4-1BB/CD3ζ ATAM (Figure 3C). From these data, the 2vv method was able to transduce ATAMs in a higher intensity than with the 1vv method. Because the ATAM and tEGFR were directly connected with the 2A sequence, the expression of ATAM and tEGFR should be equimolar.

To further investigate the effect of higher ATAM expression on intracellular signaling, we adopted an experimental system using Jurkat reporter cells.[20] These reporter cells are characterized by the stable transduction with a nuclear factor κB (NF-κB)-cyan fluorescent protein (CFP) construct; the activation of NF-κB signaling can be evaluated by quantifying the emission of CFP. We transduced 4-1BB/CD3ζ and NY-ESO-1 TCRs by the 2vv method to Jurkat reporter cells and sorted them into cells with three levels of ATAM expression intensity (Figure 4A). The expression levels of the NY-ESO-1 TCR were confirmed to be comparable after sorting (MFI of NY-ESO-1 tetramer: EGFR low, 1,037; EGFR middle, 916; EGFR high, 1,257) (Figure 4B). We analyzed emission of CFP from sorted Jurkat reporter cells stimulated with gamma-irradiated, peptide-pulsed Epstein-Barr virus (EBV)-transformed lymphoblastoid cell line (LCL) at 12, 24, 48, and 72 hours, respectively (Figure 4C). Jurkat reporter cells with high 4-1BB/CD3ζ (EGFR high) showed a higher NF-κB signal, whereas the EGFR-low and the EGFR-middle Jurkat reporter cells showed only a small difference in the NF-κB signal. To further assess more proximal signals, we performed an intracellular phosphoprotein assay. We evaluated phosphorylated (phospho-)Erk and phospho-p38 of sorted Jurkat reporter cells stimulated with peptide-pulsed LCL cells (Figures 4D and 4E). Jurkat reporter cells expressing the highest amount of ATAM had the strongest phosphorylation of the signaling moiety. Conversely, EGFR-low and EGFR-middle Jurkat cells did not exhibit much augmentation of phospho-Erk and p38. We found that the greater amount of ATAM could enhance signaling activity in the experimental system using the Jurkat reporter cell line. Furthermore, the strong signal enhancement effect was seen only in EGFR-high cells, suggesting that there may be a threshold for obtaining signal enhancement.

Comparison of CTLs Generated by Two Different Transduction Methods

Next, we compared TCR-CTLs generated by the 1vv method and 2vv method. As we observed in the experiments with Jurkat reporter cell lines, TCR-CTLs generated by the 2vv method exhibited significantly higher expression of ATAMs than did those by the 1vv method (Figures 5A and 5B). Whereas we observed the difference in EGFR expression, the TCR expressions demonstrated by the NY-ESO-1 tetramer were similar between TCR-CTLs of the 1vv method and those of the 2vv method (Figure 5A, right panel). We observed the lower tEGFR MFI in the vector with longer insertional gene length. The 4-1BB/CD3ζ group demonstrated a lower MFI. Accordingly, we considered that the insertional gene length was one of the main determinants for the expression of ATAMs. In the proliferation assay after peptide-pulsed K562-HLA-A2 stimulation, an increase in proliferative capacity due to the transduction of ATAM was observed only in the 2vv transduction method (Figure 5C). It was shown that a higher intensity of ATAM delivery allows ATAM to exert its effects.

DISCUSSION

In the present study, we attempted to develop a single virus vector to enable transducing a tumor-specific TCR and ATAM simultaneously for enhancing intracellular singling. The single virus transduction of TCR and ATAM was successful; hence, we could not observe any positive effect by the ATAM transduction.[10] In our previous study, whereas we observed no additional effect on cytotoxicity and cytokine production, a boost effect on cell proliferation was observed after antigen stimulation in the 4-1BB/CD3ζ ATAM.[10] We adopted the transduction of two separated virus vectors (2vv method) in the previous study. However, in the present study, we utilized the single virus transduction (1vv method). Thus, we compared the 1vv method and

MM.1S cells by flow cytometry analysis every 24 h were assessed. To allow ATAM$^+$ CTLs to recognize MM.1S and to separate CTLs from MM.1S cells, we transduced HLA-A2 and EGFP to MM.1S in this experiment. Representative flow plots are shown. (F) Data from (E) were summarized from three different donor CTLs. The effector and target cell fractions were obtained by flow cytometry as shown in (E). The percentages of CTLs at 48 and 120 h are shown. Data represent means ± SEM, and no significant differences were observed (one-way ANOVA).

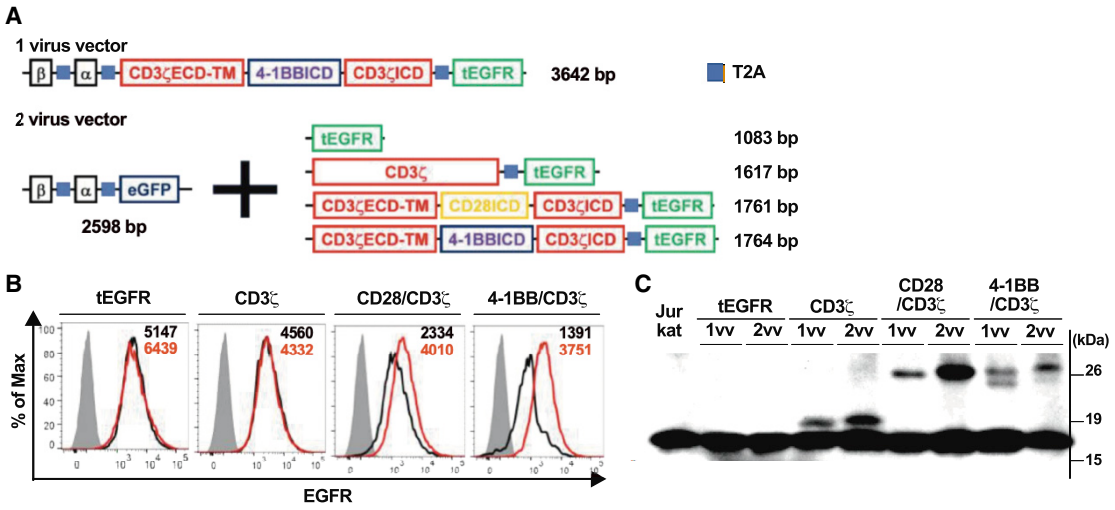

Figure 3. Comparison of ATAM-EGFR Expression after Two Different Transduction Methods in Jurkat Cell Line

(A) Schematic representation of vector constructs used in two different transduction methods. One virus-vector (1vv) constructs are the same as Figure 1A; 4-1BB/CD3ζ of 1vv constructs is exemplified. In the two virus-vector (2vv) method, an equal amount of the supernatant of two constructs is mixed and used. The numbers indicate the length of the gene insert. (B) Flow cytometry analysis of ATAM$^+$ Jurkat cell lines either after 1vv or 2vv method transduction. Gray histograms represent parallel-stained untransduced Jurkat cells. Black histograms represent 1vv method, and red histogram represent 2vv method. MFI of EGFR in 1vv and 2vv methods are shown in black and red numbers, respectively. Representative data are shown (n = 2). (C) Western blotting with anti-CD3ζ of untransduced and ATAM-transduced Jurkat cells in (B). Equal amounts of Jurkat cells were lysed and loaded. Equivalent endogenous CD3ζ staining was observed in each lane instead of a loading control. Representative data are shown (n = 2).

2vv method to elucidate the underlying mechanism of why we could not see the expected effect by the 1vv method.

In comparison between the 1vv method and 2vv method, a higher intensity of ATAM after the 2vv method than that after the 1vv method was observed in both of the Jurkat cell lines and primary T cells. Furthermore, signal intensity after antigen stimulation was associated with ATAM expression in Jurkat reporter cell experiments. In the 1vv method, the TCR and ATAM were linked with the T2A sequence, and single transduction was attempted. Alternatively, in the 2vv method, the TCR and ATAM were separately transduced with each promoter sequence, respectively. Furthermore, the total packaged gene length was also different between the 1vv method and 2vv method, such as 3.6 kb in the 1vv method, and 2.6 and 1.7 kb in the 2vv method. The gene transduction efficiency and copy number (intensity) are known to be largely dependent on the length of the gene of interest (GOI).[21] In terms of both the gene transduction efficiency and intensity, separate transduction with the 2vv method was advantageous. Nonetheless, the 2vv method is too complicated of a method when we think about practical cell production for future clinical applications. Because the gene transduction efficiency with a transposon is considered unlikely to associate with the length of the GOI,[22–24] non-viral transduction methods including the transposon method may become a solution. Alternatively, we may consider utilizing the vector system that has two separated promoter sequences to drive two individual transgenes.[25]

One of the possible reasons to explain why we could not demonstrate a 4-1BB/CD3ζ ATAM effect in the single virus vector may be due to the existence of endogenous CD3ζ. Because there was a huge amount of endogenous CD3ζ in the primary T cells, we would need to express a significant amount of ATAM to exhibit the visible effect. Otherwise, the effect of ATAM would be diluted and interference with endogenous CD3ζ would be difficult to see, even if ATAM had a good potential to boost the intracellular signals. Based on the observations in the experiments using Jurkat reporter cells, we thought that the effect of ATAM would not be linearly elevated, but it may be observed when ATAM expression would be higher than a certain threshold. Accordingly, because ATAM expression was higher in the cells produced with the 2vv method, we considered that the inhibitory effect of endogenous CD3ζ would not be seen in the 2vv method. To exclude the possibility of interference by endogenous CD3ζ, we may try to knock out the *CD3ζ* gene by genome-editing technology such as the CRISPR-Cas9 system or others.[26–28] However, the genome editing in primary T cells may bring further difficulty to make practical TCR-T cells in the clinical grade.[29]

In the present study, we demonstrated the advantage of the 2vv method in terms of transduction efficiency and intensity to exhibit the potency of ATAM. ATAM-transduced TCR-T cells demonstrated improved proliferation when ATAM was transduced in a higher intensity to TCR-T cells.

MATERIALS AND METHODS

Cell Lines

The SUP-T1 and MM.1S tumor cell lines were obtained from the American Type Culture Collection. K562, Jurkat tumor cell line, and LCL cells were maintained in our laboratory. All cell

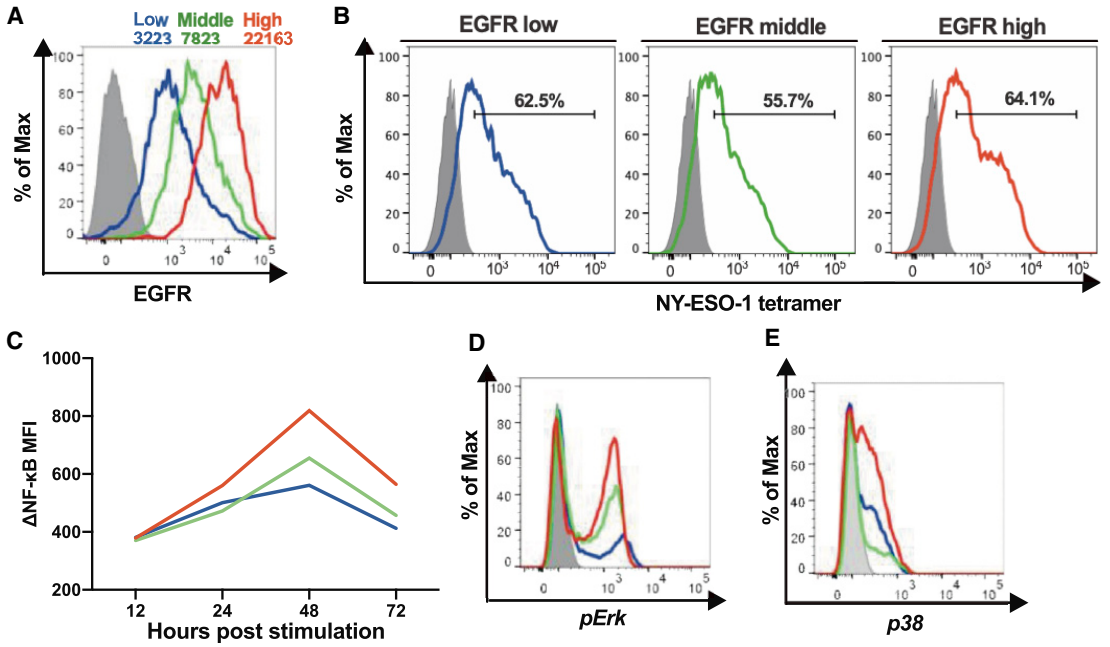

Figure 4. Association between ATAM Expression Level and Downstream Signaling Enhancement in the Jurkat Reporter Cell Line

(A) EGFR expression of ATAM$^+$ Jurkat reporter cells after being sorted. Jurkat reporter cells were transduced with TCR and 4-1BB/CD3ζ ATAM in the 2vv method, and sorted by the expression level of EGFR. Gray histograms represent parallel-stained untransduced Jurkat reporter cells. The number indicates EGFR MFI. (B) NY-ESO-1 tetramer staining of sorted ATAM$^+$ Jurkat reporter cells. (C) NF-κB activation was quantified by evaluating ECFP fluorescence of sorted Jurkat reporter cells after stimulation with peptide-pulsed LCL cells. ΔNF-κB MFI means difference of ECFP MFI between the MFI of each time point and starting point. (D and E) Intracellular phosphoprotein analysis of sorted Jurkat reporter cells after stimulation with peptide-pulsed LCL cells. Gray histograms represent parallel-stained Jurkat reporter cells stimulated with peptide-unpulsed LCL cells. pErk, phospho-Erk; p38, phospho-p38. For (A)–(E), representative results are shown from two repeated experiments with similar results. Blue histogram represents low EGFR, green represents middle EGFR, and red represents high EGFR.

lines were routinely validated for authenticity by examining their immunophenotype by flow cytometry, and culture was limited to a maximum of 2 months prior to use. K562 and MM.1S cells were tested for HLA-A2 expression by flow cytometry and NY-ESO-1 expression by RT-PCR.[10] K562 cells were HLA-A2$^-$/NY-ESO-1$^-$, and MM.1S cells were HLA-A2$^-$/NY-ESO-1$^+$. All cell lines were cultured in RPMI 1640 medium containing 10% FBS, 0.8 mmol/L L-glutamine, and 1% penicillin-streptomycin. Dr. Michael C. Jensen (Seattle Children's Research Institute, Seattle, WA, USA) kindly provided the lentivirus vector encoding GFP-firefly luciferase (ffluc). MM.1S-ffluc was derived by lentiviral transduction with the GFP-ffluc gene and was then sorted for expression of GFP.

Human Subjects

The research protocols of this study were approved by the Institutional Review Board of Nagoya University Graduate School of Medicine (reference nos. 2014-0081 and 2017-0445). Peripheral blood mononuclear cells (PBMCs) were obtained from healthy donors after written informed consent and were obtained in accordance with the Declaration of Helsinki.

ATAM Generation and Retroviral Vector Construction

We generated two ATAMs, CD28/CD3ζ and 4-1BB/CD3ζ, and prepared unmodified CD3ζ as a control in the previous study.[10] The CD28 or 4-1BB ICDs were inserted in the middle of the CD3ζ ICD such that they could assemble with the TCR complex when stimulated with the corresponding antigen. We combined the NY-ESO-1 TCR and ATAMs, and they were fused to a tEGFR lacking the epidermal growth factor-binding and intracellular signaling domains. A P2A sequence is located between the TCR α and β chains. We inserted the self-cleaving T2A sequence between the TCR, ATAM, and tEGFR. By inserting the T2A sequence, each protein was coexpressed at equimolar levels from a single transcript in a bicistronic construct.[30–32] Cell surface tEGFR was detected using the biotinylated Erbitux (cetuximab) monoclonal antibody (mAb) for EGFR (Bristol Myers Squibb, New York, NY, USA). The ATAM transgenes were assembled by overlap extension PCR. TCR-T2A-ATAM-T2A-tEGFR was packaged into LZRS-pBMN-Z using the EcoRI and NotI sites, and ATAM-encoding retrovirus was produced using the Phoenix-Ampho system (Orbigen, San Diego, CA, USA).

In the 1vv method, TCR-T2A-ATAM-T2A-tEGFR was packaged into one virus vector, and single transduction was attempted, whereas in the 2vv method, two independent virus vectors packaged as TCR-T2A-EGFP or ATAM-T2A-tEGFR were transduced simultaneously as described previously.[10] Except for the gene insert, vector backbone, promoter, and multiplicity of infection (MOI of 3) are identical between the 1vv method and 2vv method.

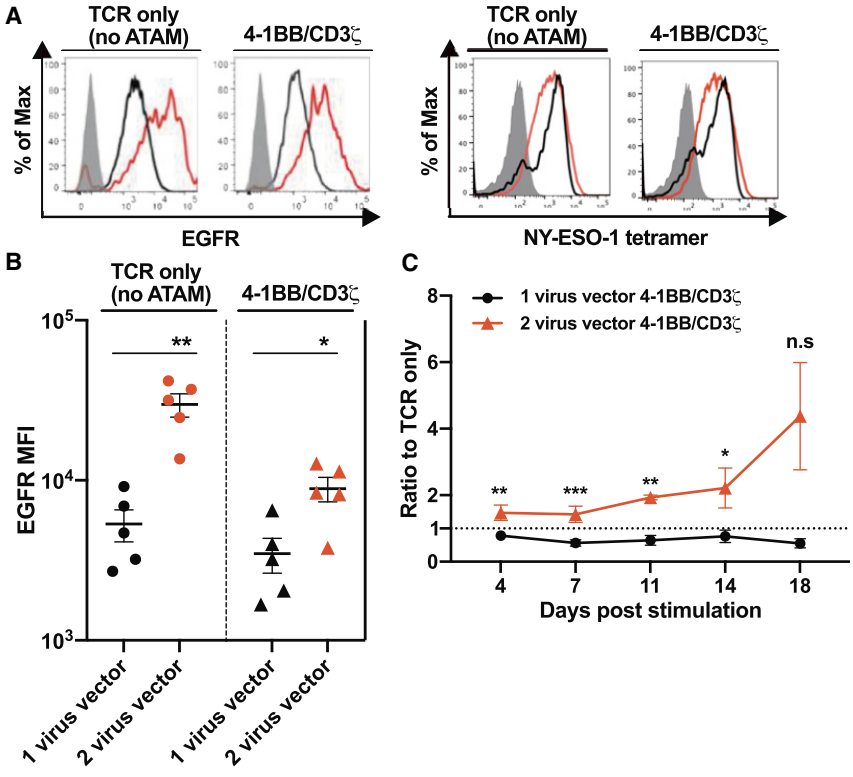

Figure 5. Comparison of 4-1BB/CD3ζ ATAM-Transduced TCR-T Cells by Two Different Transduction Methods

(A and B) Comparison of EGFR expression of ATAM$^+$ CTLs generated by either the 1vv or 2vv method. TCR, TCR-T2A-tEGFR transduced by the 1vv method, or TCR-EGFP plus tEGFR transduced by the 2vv method; 4-1BB/CD3ζ, TCR-T2A-4-1BB/CD3z-T2A-tEGFR by the 1vv method, or TCR-EGFP plus 4-1BB/CD3z-T2A-tEGFR transduced by the 2vv method. Gray histograms represent parallel-cultured and stained untransduced T cells. Representative data are shown in (A), and a summary from five different donors is shown in (B) (paired Student's t test: *$p < 0.05$; **$p < 0.01$). Data represent means ± SEM. Black histograms represent the 1vv method, and red histograms represent the 2vv method. (C) Proliferation after single antigen stimulation was assessed using standard trypan blue dye exclusion, with the data normalized to the TCR group transduced by the same virus vector method (set to 1.0). Data from the analysis of six different donors are shown. Data represent means ± SEM (paired Student's t test: *$p < 0.05$, **$p < 0.01$, ***$p < 0.001$).

Generation, Expansion, and Selection of ATAM-Transduced CTLs

We adopted the NY-ESO-1-specific TCR as a model of tumor-specific TCR gene insertion. The construct was developed based on the 1G4 TCR that targets the NY-ESO-1 peptide 157–165 (SLLMWITQC) bound to HLA-A02:01.[33] In addition, the TCR α and β chains were sterically stabilized by the additional interchain disulfide bonding.[34] CD8$^+$ T cells were purified with immunomagnetic beads (Miltenyi Biotec, Bergisch Gladbach, Germany) from healthy donor PBMCs, activated with anti-CD3/CD28 beads at the ratio of 1:1 (Invitrogen, Carlsbad, CA, USA) and cultured in RPMI 1640 medium containing 10% human serum, 0.8 mmol/L L-glutamine, 1% penicillin-streptomycin, and 0.5 μM 2-mercaptoethanol, and supplemented with recombinant human IL-2 to a final concentration of 50 IU/mL. On days 3 and 4, in the 1vv method, NY-ESO-1 TCR-ATAM-tEGFR was transduced to expanded CD8$^+$ T cells with the recombinant human fibronectin fragment (RetroNectin, Takara Bio) by centrifugation at 2,100 rpm for 120 min at 32°C with the retroviral supernatant from NY-ESO-1 TCR-ATAM-tEGFR-packaged Phoenix-Ampho cells. At 4 days after transduction, EGFR$^+$ cells were purified by biotinylated Erbitux mAb for EGFR and anti-biotin microbeads (Miltenyi Biotec). In the 2vv method, on days 3 and 4, NY-ESO-1 TCR-EGFP and ATAM-tEGFR were transduced simultaneously, using the same methods for the 1vv method. The retroviral supernatant from NY-ESO-1 TCR-EGFP and ATAM-tEGFR-packaged Phoenix-Ampho cells were mixed at a 1:1 ratio. After 4 days from transduction, NY-ESO-1 TCR$^+$ and ATAM$^+$ cells were sorted by FACSAria II, targeting the EGFP$^+$/tEGFR$^+$ fraction. Four days after selection or cell sorting, purified ATAM+NY-ESO-1 TCR-CTLs were cryopreserved. Then, we thawed CTLs and re-stimulated CTLs with gamma-irradiated LCL cells (75 Gy) pulsed with 5 μg/mL of NY-ESO-1 peptide. Thereafter, the expanded TCR-CTLs were applied for all subsequent experiments.

Flow Cytometry Analysis

All samples were analyzed by flow cytometry on the FACSAria II and FACSCanto II (BD Biosciences, San Jose, CA, USA) and analyzed using FlowJo (Tree Star, Ashland, OR, USA). The following fluorescent dye-conjugated antibodies were purchased from BD Biosciences (streptavidin-phycoerythrin [PE], CD8-PE [clone HIT8α], CD8-allophycocyanin [APC] [RPA-T8], CD3-APC [UCHT1], IL-2-APC [5344.111]), BioLegend (San Diego, CA, USA) (IFN-γ-Brilliant Violet 421 [BV421] [clone 4S.B3], HLA-A2-PE [BB7.2]), and MEDICAL & BIOLOGICAL LABORATORIES (Nagoya, Japan) (NY-ESO-1 tetramer-PE). The following antibodies were purchased from Cell Signaling Technology (Danvers, MA, USA) (phospho-p38 mitogen-activated protein kinase [MAPK] rabbit Ab [#9212], phospho-p44/42 MAPK rabbit Ab [#9101]) and BioLegend (Alexa Fluor 647 donkey anti-rabbit IgG antibody).

Intracellular Cytokine Staining and Cytokine Secretion Assay

ATAM+CTLs and K562-HLA-A2 cells pulsed with or without NY-ESO-1 peptide were mixed at a 1:1 ratio in the presence of brefeldin A (Sigma-Aldrich, St. Louis, MO, USA) and then fixed and permeabilized with cell fixation/permeabilization kits (BD Biosciences) for the intracellular cytokine assay. After fixation, CTLs were stained with CD8 mAb to separate them from stimulator cells. Anti-IFN-γ

or anti-IL-2 was used to detect intracellular cytokines. For the cytokine secretion assay, ATAM+CTLs and K562-HLA-A2 cells pulsed with or without NY-ESO-1 peptide and then mixed at a 1:1 ratio and incubated for 16 h. Culture supernatants were collected and IFN-γ or IL-2 was measured by ELISA according to the manufacturer's instructions (BD Biosciences).

CTL Proliferation Assay

ATAM+CTLs were stimulated with 100 Gy gamma-irradiated K562-HLA-A2 cells pulsed with NY-ESO-1 peptide at a 1:1 ratio and incubated at 37°C. The live cell number was assessed using standard trypan blue dye exclusion. For this assay, CTLs were cultured with 10 ng/mL IL-7 and 5 ng/mL IL-15 twice weekly.

Coculture Assay

MM.1S cells transduced with HLA-A2-EGFP were washed and plated with mock or NY-ESO-1 TCR CTLs or 4-1BB/CD3ζ-transduced NY-ESO-1 TCR CTLs at various E:T ratios, without IL-2 supplementation. From 24 to 120 h of incubation, effector cells were stained with anti-CD8 and analyzed by flow cytometry every 24 h, assessing the percentage of CTLs and MM.1S cells within the live cell gates.

Analysis of Transcription Factor and Intracellular Phosphoprotein

To generate ATAM-transduced Jurkat cells by the 2vv method, NY-ESO-1 TCR-EGFP and ATAM-tEGFR were transduced into Jurkat reporter cells simultaneously, and these cell lines were sorted as the $EGFR^+/tEGFR^+$ fraction. For ATAM-transduced Jurkat cells by the 1vv method, Jurkat cells were transduced with a single virus containing TCR-ATAM-tEGFR and sorted as the $tEGFR^+$ fraction. The reporter cells were gene modified to generate enhanced CFP (ECFP) when NF-κB was activated.[20] ATAM+Jurkat reporter cells were stimulated with LCL cells pulsed with NY-ESO-1 peptide at a 2:1 ratio, and Jurkat cells were stained with anti-CD3 and analyzed by flow cytometry at 12, 24, 48, and 72 h.

For the intracellular phosphoprotein assay, sorted Jurkat reporter cells and LCL cells pulsed with NY-ESO-1 peptide were mixed at a 1:5 ratio for 1 h, then fixed and permeabilized per the manufacturer's recommended protocol. After fixation, Jurkat cells were stained with anti-CD3 mAb to separate them from stimulator cells. Anti-phospho-p38 or anti-phospho-Erk Ab and anti-rabbit-IgG antibody were used to detect phosphorylated protein as described previously.[35]

Statistical Analysis

All experimental data are presented as mean ± SEM. Data were analyzed using paired Student's t tests to evaluate two-tailed statistical differences when comparing two groups. Differences among three or more groups were evaluated with one-way ANOVA followed by Bonferroni test. Two-way ANOVA followed by Bonferroni multiple comparison test was used to assess differences between multiple treatment groups over different time points. Statistical analysis was performed on GraphPad Prism 8 software (GraphPad, San Diego, CA, USA).

AUTHOR CONTRIBUTIONS

Conception and design: T.S. and S.T. Development of methodology: T.S. and S.T. Acquisition of data (e.g., provided animals, acquired and managed patients, provided facilities): T.S., K.M., S.T., S.O., Y.A., K.U., J.J., K.W., H.H., and H. Kishi. Analysis and interpretation of data (e.g., statistical analysis, biostatistics, computational analysis): T.S., K.M., S.T., S.O., Y.A., K.U., J.J., K.W., and T.N. Writing, review, and/or revision of the manuscript: T.S., S.T., M.M., and H. Kiyoi. Administrative, technical, or material support (i.e., reporting or organizing data, constructing databases): H.H., H. Kishi, J.L., and P.S. Study supervision: S.T., M.M., and H. Kiyoi

CONFLICTS OF INTEREST

H. Kiyoi reports grants from Chugai Pharmaceutical, Kyowa Kirin, Zenyaku Kogyo, Fujifilm, Otsuka Pharmaceutical, Takeda Pharmaceutical, Sumitomo Dainippon Pharma, Sanofi, Celgene, Nippon Shinyaku, Eisai, and Pfizer Japan; grants and personal fees from Daiichi Sankyo, Astellas, and Novartis Pharma; and personal fees from Bristol Myers Squibb and Amgen Astellas BioPharma that are all unrelated to the submitted work. The remaining authors declare no competing interests.

ACKNOWLEDGMENTS

The authors would like to thank members of the Division of Experimental Animals and the Division of Medical Research Engineering, Nagoya University Graduate School of Medicine for technical assistance. This work was supported by grants from the Japan Society for the Promotion of Science (JSPS) KAKENHI (15k09497 and 18k08351 to S.T.), Practical Research for Innovative Cancer Control (15ck0106067h0002 and 17ck0106291h0001 to S.T.), and Practical Research Project for Allergic Diseases and Immunology (19ek0510022h0003 to S.T. and M.M.). J.J. was supported by a grant from the Research Foundation of Prince of Songkla University (no. MOE.0521.1.0601(2)/6058).

REFERENCES

1. Stauss, H.J., Cesco-Gaspere, M., Thomas, S., Hart, D.P., Xue, S.A., Holler, A., Wright, G., Perro, M., Little, A.M., Pospori, C., et al. (2007). Monoclonal T-cell receptors: new reagents for cancer therapy. Mol. Ther. *15*, 1744–1750.

2. Spear, T.T., Evavold, B.D., Baker, B.M., and Nishimura, M.I. (2019). Understanding TCR affinity, antigen specificity, and cross-reactivity to improve TCR gene-modified T cells for cancer immunotherapy. Cancer Immunol. Immunother. *68*, 1881–1889.

3. Leung, W., and Heslop, H.E. (2019). Adoptive immunotherapy with antigen-specific T cells expressing a native TCR. Cancer Immunol. Res. *7*, 528–533.

4. D'Ippolito, E., Schober, K., Nauerth, M., and Busch, D.H. (2019). T cell engineering for adoptive T cell therapy: safety and receptor avidity. Cancer Immunol. Immunother. *68*, 1701–1712.

5. Tawara, I., Kageyama, S., Miyahara, Y., Fujiwara, H., Nishida, T., Akatsuka, Y., Ikeda, H., Tanimoto, K., Terakura, S., Murata, M., et al. (2017). Safety and persistence of WT1-specific T-cell receptor gene-transduced lymphocytes in patients with AML and MDS. Blood *130*, 1985–1994.

6. Foley, K.C., Spear, T.T., Murray, D.C., Nagato, K., Garrett-Mayer, E., and Nishimura, M.I. (2017). HCV T cell receptor chain modifications to enhance expression, pairing, and antigen recognition in T cells for adoptive transfer. Mol. Ther. Oncolytics *5*, 105–115.

7. Morgan, R.A., Dudley, M.E., Wunderlich, J.R., Hughes, M.S., Yang, J.C., Sherry, R.M., Royal, R.E., Topalian, S.L., Kammula, U.S., Restifo, N.P., et al. (2006). Cancer regression in patients after transfer of genetically engineered lymphocytes. Science *314*, 126–129.

8. Robbins, P.F., Morgan, R.A., Feldman, S.A., Yang, J.C., Sherry, R.M., Dudley, M.E., Wunderlich, J.R., Nahvi, A.V., Helman, L.J., Mackall, C.L., et al. (2011). Tumor regression in patients with metastatic synovial cell sarcoma and melanoma using genetically engineered lymphocytes reactive with NY-ESO-1. J. Clin. Oncol. *29*, 917–924.

9. Chandran, S.S., Paria, B.C., Srivastava, A.K., Rothermel, L.D., Stephens, D.J., Dudley, M.E., Somerville, R., Wunderlich, J.R., Sherry, R.M., Yang, J.C., et al. (2015). Persistence of CTL clones targeting melanocyte differentiation antigens was insufficient to mediate significant melanoma regression in humans. Clin. Cancer Res. *21*, 534–543.

10. Miyao, K., Terakura, S., Okuno, S., Julamanee, J., Watanabe, K., Hamana, H., Kishi, H., Sakemura, R., Koyama, D., Goto, T., et al. (2018). Introduction of genetically modified CD3ζ improves proliferation and persistence of antigen-specific CTLs. Cancer Immunol. Res. *6*, 733–744.

11. Abate-Daga, D., and Davila, M.L. (2016). CAR models: next-generation CAR modifications for enhanced T-cell function. Mol. Ther. Oncolytics *3*, 16014.

12. Kowolik, C.M., Topp, M.S., Gonzalez, S., Pfeiffer, T., Olivares, S., Gonzalez, N., Smith, D.D., Forman, S.J., Jensen, M.C., and Cooper, L.J. (2006). CD28 costimulation provided through a CD19-specific chimeric antigen receptor enhances in vivo persistence and antitumor efficacy of adoptively transferred T cells. Cancer Res. *66*, 10995–11004.

13. Call, M.E., and Wucherpfennig, K.W. (2004). Molecular mechanisms for the assembly of the T cell receptor-CD3 complex. Mol. Immunol. *40*, 1295–1305.

14. Varma, R., Campi, G., Yokosuka, T., Saito, T., and Dustin, M.L. (2006). T cell receptor-proximal signals are sustained in peripheral microclusters and terminated in the central supramolecular activation cluster. Immunity *25*, 117–127.

15. Huppa, J.B., Gleimer, M., Sumen, C., and Davis, M.M. (2003). Continuous T cell receptor signaling required for synapse maintenance and full effector potential. Nat. Immunol. *4*, 749–755.

16. Maus, M.V., Grupp, S.A., Porter, D.L., and June, C.H. (2014). Antibody-modified T cells: CARs take the front seat for hematologic malignancies. Blood *123*, 2625–2635.

17. Okamoto, S., Amaishi, Y., Goto, Y., Ikeda, H., Fujiwara, H., Kuzushima, K., Yasukawa, M., Shiku, H., and Mineno, J. (2012). A promising vector for TCR gene therapy: differential effect of siRNA, 2A peptide, and disulfide bond on the introduced TCR expression. Mol. Ther. Nucleic Acids *1*, e63.

18. Echchannaoui, H., Petschenka, J., Ferreira, E.A., Hauptrock, B., Lotz-Jenne, C., Voss, R.H., and Theobald, M. (2019). A potent tumor-reactive p53-specific single-chain TCR without on- or off-target autoimmunity in vivo. Mol. Ther. *27*, 261–271.

19. Bendle, G.M., Linnemann, C., Hooijkaas, A.I., Bies, L., de Witte, M.A., Jorritsma, A., Kaiser, A.D.M., Pouw, N., Debets, R., Kieback, E., et al. (2010). Lethal graft-versus-host disease in mouse models of T cell receptor gene therapy. Nat. Med. *16*, 565–570.

20. Jutz, S., Leitner, J., Schmetterer, K., Doel-Perez, I., Majdic, O., Grabmeier-Pfistershammer, K., Paster, W., Huppa, J.B., and Steinberger, P. (2016). Assessment of costimulation and coinhibition in a triple parameter T cell reporter line: Simultaneous measurement of NF-κB, NFAT and AP-1. J. Immunol. Methods *430*, 10–20.

21. Velu, T.J., Beguinot, L., Vass, W.C., Zhang, K., Pastan, I., and Lowy, D.R. (1989). Retroviruses expressing different levels of the normal epidermal growth factor receptor: biological properties and new bioassay. J. Cell. Biochem. *39*, 153–166.

22. Balciunas, D., Wangensteen, K.J., Wilber, A., Bell, J., Geurts, A., Sivasubbu, S., Wang, X., Hackett, P.B., Largaespada, D.A., McIvor, R.S., and Ekker, S.C. (2006). Harnessing a high cargo-capacity transposon for genetic applications in vertebrates. PLoS Genet. *2*, e169.

23. Huang, X., Guo, H., Tammana, S., Jung, Y.C., Mellgren, E., Bassi, P., Cao, Q., Tu, Z.J., Kim, Y.C., Ekker, S.C., et al. (2010). Gene transfer efficiency and genome-wide integration profiling of *Sleeping Beauty*, *Tol2*, and *piggyBac* transposons in human primary T cells. Mol. Ther. *18*, 1803–1813.

24. Tipanee, J., VandenDriessche, T., and Chuah, M.K. (2017). Transposons: moving forward from preclinical studies to clinical trials. Hum. Gene Ther. *28*, 1087–1104.

25. Dastpak, M., Matin, M.M., Farshchian, M., Arsenijevic, Y., Momeni-Moghaddam, M., Sisakhtnezhad, S., Boozarpour, S., Bidkhori, H.R., Mirahmadi, M., and Bahrami, A.R. (2014). Construction and quantitative evaluation of a dual specific promoter system for monitoring the expression status of *Stra8* and *c-kit* genes. Mol. Biotechnol. *56*, 1100–1109.

26. Lee, M., and Kim, H. (2019). Therapeutic application of the CRISPR system: current issues and new prospects. Hum. Genet. *138*, 563–590.

27. Bailey, S.R., and Maus, M.V. (2019). Gene editing for immune cell therapies. Nat. Biotechnol. *37*, 1425–1434.

28. Gautron, A.S., Juillerat, A., Guyot, V., Filhol, J.M., Dessez, E., Duclert, A., Duchateau, P., and Poirot, L. (2017). Fine and predictable tuning of TALEN gene editing targeting for improved T cell adoptive immunotherapy. Mol. Ther. Nucleic Acids *9*, 312–321.

29. Mastaglio, S., Genovese, P., Magnani, Z., Ruggiero, E., Landoni, E., Camisa, B., Schiroli, G., Provasi, E., Lombardo, A., Reik, A., et al. (2017). NY-ESO-1 TCR single edited stem and central memory T cells to treat multiple myeloma without graft-versus-host disease. Blood *130*, 606–618.

30. Wang, X., Chang, W.C., Wong, C.W., Colcher, D., Sherman, M., Ostberg, J.R., Forman, S.J., Riddell, S.R., and Jensen, M.C. (2011). A transgene-encoded cell surface polypeptide for selection, in vivo tracking, and ablation of engineered cells. Blood *118*, 1255–1263.

31. Watanabe, K., Terakura, S., Martens, A.C., van Meerten, T., Uchiyama, S., Imai, M., Sakemura, R., Goto, T., Hanajiri, R., Imahashi, N., et al. (2015). Target antigen density governs the efficacy of anti-CD20-CD28-CD3 ζ chimeric antigen receptor-modified effector $CD8^+$ T cells. J. Immunol. *194*, 911–920.

32. Paszkiewicz, P.J., Fräßle, S.P., Srivastava, S., Sommermeyer, D., Hudecek, M., Drexler, I., Sadelain, M., Liu, L., Jensen, M.C., Riddell, S.R., and Busch, D.H. (2016). Targeted antibody-mediated depletion of murine CD19 CAR T cells permanently reverses B cell aplasia. J. Clin. Invest. *126*, 4262–4272.

33. Cohen, C.J., Li, Y.F., El-Gamil, M., Robbins, P.F., Rosenberg, S.A., and Morgan, R.A. (2007). Enhanced antitumor activity of T cells engineered to express T-cell receptors with a second disulfide bond. Cancer Res. *67*, 3898–3903.

34. Robbins, P.F., Li, Y.F., El-Gamil, M., Zhao, Y., Wargo, J.A., Zheng, Z., Xu, H., Morgan, R.A., Feldman, S.A., Johnson, L.A., et al. (2008). Single and dual amino acid substitutions in TCR CDRs can enhance antigen-specific T cell functions. J. Immunol. *180*, 6116–6131.

35. Terakura, S., Yamamoto, T.N., Gardner, R.A., Turtle, C.J., Jensen, M.C., and Riddell, S.R. (2012). Generation of CD19-chimeric antigen receptor modified $CD8^+$ T cells derived from virus-specific central memory T cells. Blood *119*, 72–82.